LETTER

https://doi.org/10.1038/s41586-018-0045-y

Earthquake–induced transformation of the lower crust

Bjørn Jamtveit[1]*, Yehuda Ben-Zion[2], François Renard[1,3] & Håkon Austrheim[1]

The structural and metamorphic evolution of the lower crust has direct effects on the lithospheric response to plate tectonic processes involved in orogeny, including subsidence of sedimentary basins, stability of deep mountain roots and extension of high-topography regions. Recent research shows that before orogeny most of the lower crust is dry, impermeable and mechanically strong[1]. During an orogenic event, the evolution of the lower crust is controlled by infiltration of fluids along localized shear or fracture zones. In the Bergen Arcs of Western Norway, shear zones initiate as faults generated by lower-crustal earthquakes. Seismic slip in the dry lower crust requires stresses at a level that can only be sustained over short timescales or local weakening mechanisms. However, normal earthquake activity in the seismogenic zone produces stress pulses that drive aftershocks in the lower crust[2]. Here we show that the volume of lower crust affected by such aftershocks is substantial and that fluid-driven associated metamorphic and structural transformations of the lower crust follow these earthquakes. This provides a 'top-down' effect on crustal geodynamics and connects processes operating at very different timescales.

The structural and metamorphic evolutions of the lower crust are key elements in the dynamics of the lithosphere. Frequent observations of fluid-induced metamorphism associated with ductile deformation along shear zones on scales ranging from millimetres to kilometres inspired early models of the lithosphere such as the 'jelly-sandwich' model[3]. In this model, the lower crust is assumed to be wet and mechanically weak, and plate tectonic stress is transmitted through the brittle upper crust and a strong upper mantle. This model was challenged[4] with the argument that a strong lower crust is essential for the survival of thick mountain roots and high mountains. The lower crust is dominated by granulite facies rocks of mafic to intermediate composition[5] and such rocks will be nominally dry at normal steady-state geothermal gradients for a wide range of crustal heat flow and heat production conditions[1]. Hence, the rheology of the lower crust before an orogeny will in most cases be controlled by the properties of dry mineral assemblages dominated by plagioclase, pyroxene, garnet and olivine, with plagioclase being the most abundant phase. This is consistent with the estimated viscosity of the lower crust ($\geq 10^{24}$ Pa s) required to generate the crustal support needed for intraplate seismicity such as the Bhuj earthquake[6] in western India in 2001 of moment magnitude $M_w = 7.6$. Recent modelling[7] furthermore suggests that the Indian lower crust remains strong beneath the entire southern half of the Tibetan plateau.

Observations of structural and metamorphic transformation of initially dry lower crust during orogenic events indicate an early stage involving seismic failures[8–10]. Metamorphism and shear zone development then follow in the wake of lower-crustal earthquakes. These observations raise an enigma that has so far been unresolved, because frictional failure of dry rocks at the confining pressures of the lower crust (≥ 1 GPa) requires differential stress levels[11] exceeding 2 GPa. Although dry plagioclase-dominated rocks deforming by dislocation creep can in theory develop extremely high differential stress at lower-crustal temperatures and high strain rates, the stress level that can be sustained over orogenic timescales for reasonable strain rates in coherent crustal volumes will be far below what is required for brittle faulting (< 1 GPa; see Methods). Deep crustal earthquakes occurring under constant loading in intact rocks thus seem to require a local weakening mechanism.

During subduction of the Indian plate under south Tibet, earthquakes occur at 60–100 km depth (Fig. 1), but are confined to regions very close to the Mohorovičić discontinuity (Moho) at temperatures[7] below 600 °C. Interestingly, the pressure and temperature conditions in the region where these earthquakes nucleate overlap the conditions at which serpentine breaks down to produce hydrous fluids in mantle rocks. Fluid production near the Moho can both reduce effective pressures and weaken the crust and mantle by mineral transformation processes and thus it is a plausible explanation for the observed seismic activity.

In the absence of such local weakening mechanisms, seismic deformation in the lower crust may be driven by transient 'stress pulses'[6,10,12]. Here we propose that earthquakes in the brittle upper crust provide a natural mechanism for sustained generation of stress pulses and associated seismic failures in the lower crust. During the occurrence of large earthquakes the strain rates around and below the rupture area increase by many orders of magnitude. A representative strain accumulation of 15 mm per year across a width comparable to a geodetic locking depth of 15 km corresponds to an interseismic strain rate of 3×10^{-14} s^{-1}. In contrast, seismic slip velocities of 1–10 m s^{-1} across a rupture localization width of 1–10 mm lead to seismic strain rates of 10^3–10^4 s^{-1}. Such large co-seismic jumps can explain a transient increase in seismic rupture within the lower crust.

Observational evidence for very high, short-lived stresses in the lower crust come from the occurrence of fossil earthquakes. A recent study of the Woodroffe Thrust located within the Musgrave Block in central Australia[13] documents the formation of large volumes of pseudotachylytes in completely dry lower-crustal granulites. Stress levels exceeding 0.5 GPa have also been inferred from lower-crustal earthquakes, leading to pseudotachylyte formation in gabbros and ultramafic rocks in the Alpine subduction complex of Corsica, France[14].

Simulated deformation on faults using various versions of rate- and state-dependent friction models show that large earthquake slip penetrates into the nominally stable deeper regions of the crust[15,16]. Simulations of aftershocks in a viscoelastic damage model consisting of a brittle upper crust over a lower crust with power-law viscosity constrained by laboratory experiments indicate that the hypocentres of early aftershocks are deeper than the regular seismogenic zone[2]. Depending on model parameters and thermal gradients, the maximum depth of the early aftershocks can approach twice that of the usual seismicity. Details of these results depend on the constitutive laws and parameters used, but lower-crustal aftershocks are generic outcomes of the high strain rates generated by large earthquakes at the bottom of the seismogenic zone.

[1]Physics of Geological Processes (PGP), The Njord Centre, Department of Geosciences, University of Oslo, Oslo, Norway. [2]Department of Earth Sciences, University of Southern California, Los Angeles, CA, USA. [3]Université Grenoble Alpes, Université Savoie Mont Blanc, CNRS, IRD, IFSTTAR, ISTerre, Grenoble, France. *e-mail: bjorn.jamtveit@geo.uio.no

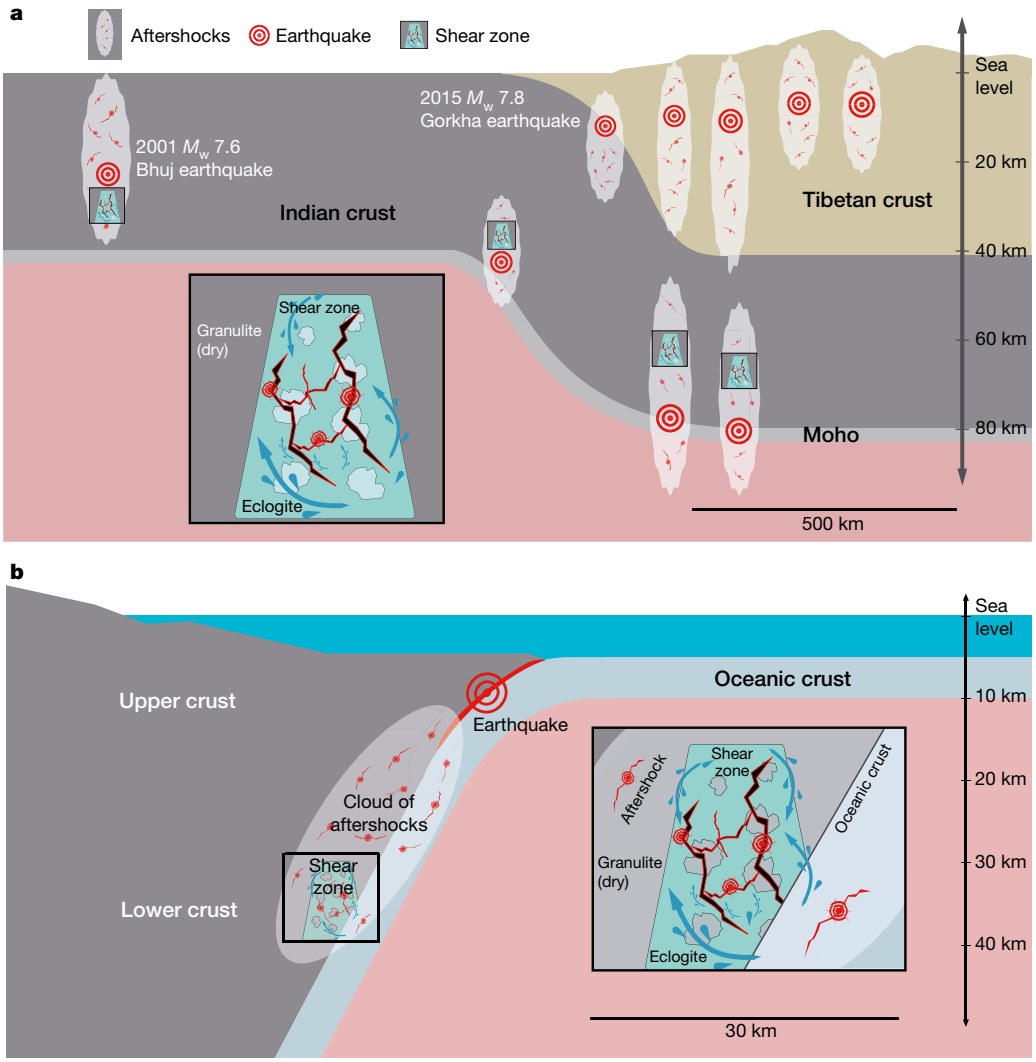

Fig. 1 | Earthquakes and aftershocks in the lower crust. a, Schematic representation of earthquakes and aftershocks for the India–Tibet continent–continent collision. Inset, enlarged shear zone. **b**, A generic subduction plate boundary geometry. Each major earthquake generates a cloud of aftershocks, some of which are in the lower crust (many aftershocks in the upper crust are not shown in these simple diagrams). These aftershocks create pathways for fluids (blue arrows in insets), allowing partial hydration and metamorphism of the strong and dry granulites into wet and weaker eclogites and amphibolites. This process also facilitates the development of shear zones in the continental lower crust. For the subduction geometry, fluids could originate from the slab below or from the upper crust above. For the continental collision below the Himalayas, fluids introduced to the subducted Indian plate could originate from the dehydration of serpentine rocks below. The 2001 Bhuj[6] and 2015 Gorkha[28] earthquakes both have aftershock 'clouds' propagating down to the lower crust, potentially allowing downward migration of fluids from the upper crust.

Below we use basic scaling relations to demonstrate that observed worldwide earthquake activity in the regular seismogenic zone of subduction zones and seismically active continental regions is expected to produce considerable fracture area and rupture zone volume in the lower crust. This, in turn, generates transient pathways for fluids from the wet upper crust above, or the slab below, to the dry lower crust (Fig. 1). Fluids have a key role in the long-term evolution of the lower crust[1]. As an example, we describe earthquake-triggered eclogite-facies metamorphism and shear zone development of lower-crustal granulites from the Bergen Arcs in Western Norway (Fig. 2a). The observations highlight the close association between earthquakes, fluid migration and transformation processes in the lower crust.

The Bergen Arcs represent a series of thrust sheets where granulite facies remnants of Proterozoic lower crust recrystallized to an anhydrous mineralogy 930 million years ago[17]. During the Caledonian continent collision between Laurentia and Baltica between 420 and 440 million years ago[17], fluid-induced metamorphic transformations formed eclogites and amphibolites in shear zones, breccias and along fractures. The estimated eclogitization conditions[18] are about 670–690 °C and 2.1–2.2 GPa. Pseudotachylytes, fine-grained or glassy fault rocks believed to reflect earthquake-related frictional melting are abundant on faults where granulites facies rocks experienced Caledonian retrograde metamorphism (Fig. 2a). Such faults show single rupture displacements reaching 1.7 m (Fig. 2b), corresponding to an earthquake exceeding magnitude 7. Single pseudotachylyte veins range in thickness from millimetres to a few centimetres (Fig. 2c), and also occur as a thin 'matrix' between rotated blocks of brecciated granulite that sometimes cover areas exceeding 100 m^2. Microstructures developing in the fault wall rocks display intense fragmentation with no, or very minor, shear strain[19], followed by healing processes through grain growth and formation of eclogite facies minerals, including hydrous phases such as amphibole, mica and clinozoisite. Infiltration of hydrous fluids is thus directly associated with seismic slip.

A substantial rheological weakening associated with formation of the fine-grained and hydrous eclogite often leads to development of ductile shear zones in areas initially deformed by brittle failure. Relict pseudotachylytes can occasionally be observed 'floating' in the shear

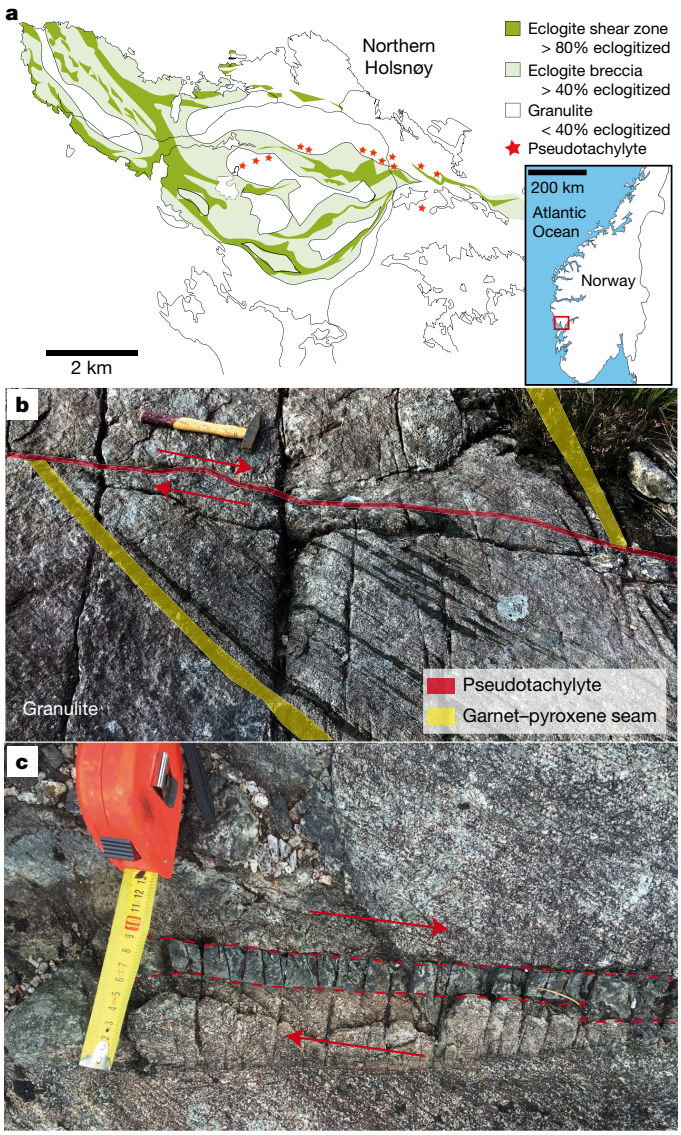

Fig. 2 | Fossil earthquakes in the Bergen Arcs. a, Map (modified from ref. [33], Elsevier) of the northwestern part of Holsnøy island in the Bergen Arcs, Western Norway, showing the location of pseudotachylytes (red stars) recording numerous fossil earthquakes near the transition between 940-million-year-old dry lower-crustal granulites and hydrated 430-million-year-old eclogites. **b**, Offset of a pyroxene-rich seam by a single lower-crustal earthquake. The slip surface is decorated with a melt layer (pseudotachylyte) indicative of seismic slip. An offset of 1.7 m corresponds to a fossil earthquake with moment magnitude $M_w \geq 7$ based on the scaling relations provided in ref. [29]. **c**, Higher-resolution image of the centimetres-thick melt layer between the two red dashed lines. Red arrows indicate the sense of slip. Photographs in **b** and **c** taken by B.J.

zones, providing unambiguous evidence for ductile deformation predated by brittle failure of granulite facies rocks (Fig. 3). In the following, we explore the feasibility that lower-crustal earthquakes, such as those described, are aftershocks triggered by stress pulses generated by mainshocks in the normal seismogenic regime of a plate boundary.

Basic seismological scaling relations provide an order-of-magnitude estimate of the lower-crustal rock volume affected by aftershocks. We show that this is substantial, with conservative parameter values and ignoring probable contributions from penetration of large mainshocks into the lower crust as well as ductile/thermal instabilities[15,16].

Lower-crustal earthquakes are not expected to occur repeatedly in the same location because rock melting and subsequent solidification is a strengthening process[20]. This is consistent with observations of distributed 'fields' of pseudotachylytes (Fig. 2a), each associated with

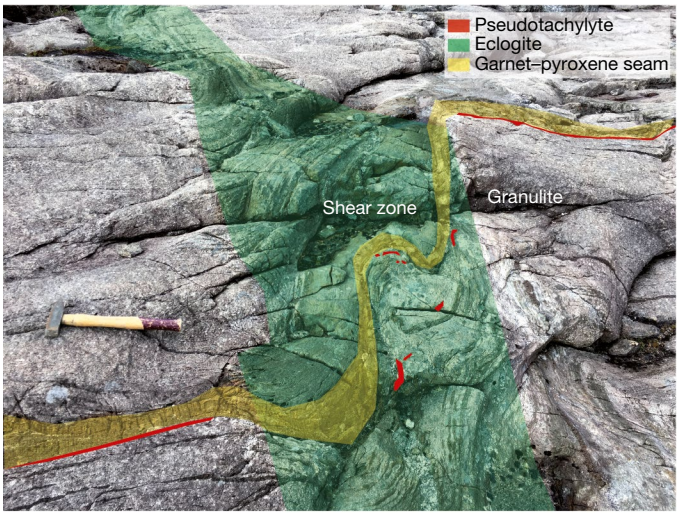

Fig. 3 | Transformation of the lower crust. Offset of a pseudotachylyte by a shear zone where dry granulite rocks are transformed into wet eclogites. The earthquake occurred before the eclogitization and probably created the pathways for fluids that triggered rock transformation. We note the remains of the pseudotachylyte inside the eclogite shear zone. Photograph taken by F.R.

a single event. The total volume of rock damage V_{rd} produced by crustal earthquakes in the magnitude range $M_1 < M < M_2$ is then given by

$$V_{rd} = \int_{M_1}^{M_2} A(M)\, t_{rd}(M)\, n(M)\, dM \quad (1)$$

Here $A(M)$ is the rupture area of an earthquake with magnitude M, $t_{rd}(M)$ is the damage zone thickness around the rupture area and $n(M)$ is the event density given by the Gutenberg–Richter relationship

$$\log_{10} n(M) = a - bM \quad (2)$$

where a and b are empirical constants. The scaling relations for $A(M)$ and $t_{rd}(M)$ are found using basic theoretical relations from fracture mechanics[21,22] and empirical relation between the magnitude and potency of earthquakes[23,24] (see Methods). An explicit relationship for the total volume of damage produced by earthquakes in the considered magnitude range can be expressed as:

$$V_{rd}(M_1 < M < M_2) = \beta[e^{\alpha M_2} - e^{\alpha M_1}] \quad (3)$$

where α and β are positive parameters that account for the combined scaling relations[21–24] of A, t_{rd} and n with M. By using observationally constrained parameters, the volume of rock damaged by crustal earthquakes is estimated to be $V_{rd} = 1.2 \times 10^{-5}$ km^3 per year per square kilometre of the Earth's surface in the seismically active region (see Methods). For the lower-magnitude limit, we use $M_1 = 0$ with slip distance of the order of the grain size of granulites. For an upper limit relevant to the lower crust, we take $M_2 = 8.3$ since the largest subduction zones events can have $M \geq 9.5$, and the largest aftershock magnitude is typically about 1.2 units below that of the mainshock[25,26]. The parameters of the Gutenberg–Richter relationship are taken from recent analysis of global earthquakes with depths[27] of less than 70 km. Analysis of earthquake clusters indicates[26,27] that about 75% of all events with $M > 0$ are aftershocks. We therefore use 75% of the observed intensity of events[27] to estimate the average annual production of damaged rock volume by aftershocks with $0 < M < 8.3$. On the basis of previously conducted simulations[2], we assume conservatively that 1% of the aftershock population is in the lower crust. The estimated annual production of rupture zone volume in the lower crust is then 1.2×10^{-7} km^3 yr^{-1} per square kilometre of the Earth's surface.

As a concrete example, Western Norway was an active subduction zone during the Caledonian orogeny for more than two million years. From the estimates above, the total seismically damaged volume in the lower crust of Western Norway is estimated to be 0.24 km^3 per square kilometre of the Earth's surface. For a 20-km-thick lower crust, this implies a rupture zone volume exceeding 1.2% of the total lower-crustal volume. The Bergen Arcs example demonstrates that in the presence of fluids, lower-crustal earthquakes initiate metamorphism of rock volumes typically 1–2 orders of magnitude larger than that of the rupture zone (that is, a 0.1–1-m-thick eclogite forming around the 1-cm-thick rupture zone). Hence, the overall process can alter a large fraction of the lower crust. The sensitivity of the results to input parameters is discussed in the Methods and shows that the 1.2% estimate of lower-crust volume damaged by earthquakes is based on conservative values of input parameters and is likely to be higher.

Our results indicate that aftershocks triggered by major earthquakes in the regular seismogenic zone have the potential to initiate pervasive transformation of the lower crust on a timescale of a million years. Direct recording of a transient deepening of early aftershocks requires a dense observational network around large mainshock ruptures. Although this situation is not often met, such lower-crust aftershocks are sometimes observed. Recent examples of deep aftershocks include the 2001 $M_w = 7.6$ Bhuj intraplate earthquake in India where aftershocks occurred down to Moho depths[6], and the 2015 $M_w = 7.8$ Gorkha earthquake in Nepal where the hypocentre occurred near the Main Himalayan Thrust at a depth[28] of 10–15 km and aftershocks penetrated the Indian crust to a depth exceeding 30 km (Fig. 1a).

Earthquakes in dry lower crust driven by stress pulses generated in the seismogenic zone have a number of important consequences, many of which are illustrated by the Bergen Arcs example. The most important is arguably the associated increase in permeability, which may connect the dry lower crust to an external fluid reservoir. In the Bergen Arcs, pseudotachylyte formation is always associated with an influx of hydrous fluids[29]. Fluid-driven metamorphic reactions are fast owing to the metastable state of the granulite facies rocks[1], leading to a profound reduction in rock strength and the development of shear zones and ductile deformation at lower stress levels[30,31]. The positive feedbacks between fluid introduction, weakening and shear zone development eventually produce a complete transformation of large volumes of lower crust from a dry and strong lithology to a wet and weak lithology. Thus even in situations where aftershocks directly affect only limited volumes of lower crust, they may start a series of fluid-induced transformation processes which can affect far bigger volumes.

The 'top-down' control on lower-crustal evolution presented here challenges the traditional 'bottom-up' view in which deep shear zones are assumed to control the spatial distribution of faults above the brittle–ductile transition. The generation of deep crustal shear zones as a response to weakening induced by pre-existing faults triggered by stress pulses generated by shallower earthquakes may also explain observed fluids with meteoric and other upper crustal signatures, such as the presence of hydrocarbons, in shear zones formed below the brittle–ductile transition[32].

Online content

Any Methods, including any statements of data availability and Nature Research reporting summaries, along with any additional references and Source Data files, are available in the online version of the paper at https://doi.org/10.1038/s41586-018-0045-y.

Received: 26 September 2017; Accepted: 22 February 2018;
Published online 25 April 2018.

1. Jamtveit, B., Austrheim, H. & Putnis, A. Disequilibrium metamorphism of stressed lithosphere. *Earth Sci. Rev.* **154**, 1–13 (2016).
2. Ben-Zion, Y. & Lyakhovsky, V. Analysis of aftershocks in a lithospheric model with seismogenic zone governed by damage rheology. *Geophys. J. Int.* **165**, 197–210 (2006).
3. Chen, W. P. & Molnar, P. Focal depths of intracontinental and intraplate earthquakes and their implication for the thermal and mechanical properties of the lithosphere. *J. Geophys. Res.* **88**, 4183–4214 (1983).
4. Jackson, J. Strength of the continental lithosphere: time to abandon the jelly sandwich? *GSA Today* **12**, 4–9 (2002).
5. Rudnick, R. L. & Fountain, D. M. Nature and composition of the continental lower crust. *Rev. Geophys.* **33**, 267–309 (1995).
6. Copley, A., Avouac, J.-P., Hollingsworth, J. & Leprince, S. The 2001 M_W 7.6 Bhuj earthquake, low fault friction and the upper crustal support of plate driving forces in India. *J. Geophys. Res.* **116**, B08405 (2011).
7. Craig, T. J., Copley, A. & Jackson, J. Thermal and tectonic consequences of India underthrusting Tibet. *Earth Planet. Sci. Lett.* **353–354**, 231–239 (2012).
8. Austrheim, H. & Boundy, T. M. Pseudotachylytes generated during seismic faulting and eclogitization of the deep crust. *Science* **265**, 82–83 (1994).
9. John, T. & Schenk, V. Interrelations between intermediate-depth earthquakes and fluid flow within subducting oceanic plates: constraints from eclogite facies pseudotachylytes. *Geology* **34**, 557–560 (2006).
10. Moecher, D. P. & Steltenpohl, M. G. Direct calculation of rupture depth for an exhumed paleoseismogenic fault from mylonitic pseudotachylyte. *Geology* **37**, 999–1002 (2009).
11. Kohlstedt, D. L., Evans, B. & Mackwell, S. J. Strength of the lithosphere—constraints imposed by laboratory experiments. *J. Geophys. Res.* **100**, 17587–17602 (1995).
12. Ellis, S. & Stöckhert, B. Elevated stresses and creep rates beneath the brittle-ductile transition caused by seismic faulting in the upper crust. *J. Geophys. Res.* **109**, B05407 (2004).
13. Hawemann, F., Mancktelow, N. S., Wex, S., Camacho, A. & Pennaccioni, G. Pseudotachylyte as field evidence for lower crustal earthquakes during the intracontinental Petermann Orogeny (Musgrave Block, Central Australia). *Solid Earth Discuss.* (submitted); preprint at https://doi.org/10.5194/se-2017-123 (2018).
14. Andersen, T. B., Mair, K., Austrheim, H., Podladchikov, Y. Y. & Vrijmoed, J. C. Stress release in exhumed intermediate and deep earthquakes determined from ultramafic pseudotachylite. *Geology* **36**, 995–998 (2008).
15. Hillers, G., Ben-Zion, Y. & Mai, P. M. Seismicity on a fault controlled by rate- and state dependent friction with spatial variations of the critical slip distance. *J. Geophys. Res.* **111**, B01403 (2006).
16. Jiang, J. & Lapusta, N. Connecting depth limits of interseismic locking, microseismicity, and large earthquakes in models of long-term fault slip. *J. Geophys. Res.* **122**, 6491–6523 (2017).
17. Bingen, B., Davis, W. J. & Austrheim, H. Zircon U-Pb geochronology in the Bergen arc eclogites and their Proterozoic protoliths, and implications for the pre-Scandian evolution of the Caledonides in western Norway. *Geol. Soc. Am. Bull.* **113**, 640–649 (2001).
18. Bhowany, K. et al. Phase equilibria modelling constraints on P-T conditions during fluid catalysed conversion of granulite to eclogite in the Bergen Arcs, Norway. *J. Metamorph. Geol.* **36**, 315–342 (2018).
19. Austrheim, H. et al. Microstructural records of seismic slip. *Sci. Adv.* **3**, e1602067 (2017).
20. Mitchell, T. M., Toy, V., Di Toro, G., Renner, J. & Sibson, R. H. Fault welding by pseudotachylyte formation. *Geology* **44**, 1059–1062 (2016).
21. Ben-Zion, Y. Collective behavior of earthquakes and faults: continuum-discrete transitions, progressive evolutionary changes and different dynamic regimes. *Rev. Geophys.* **46**, RG4006 (2008).
22. Ben-Zion, Y. & Ampuero, J.-P. Seismic radiation from regions sustaining material damage. *Geophys. J. Int.* **178**, 1351–1356 (2009).
23. Ben-Zion, Y. & Zhu, L. Potency-magnitude scaling relations for southern California earthquakes with $1.0 < M_L < 7.0$. *Geophys. J. Int.* **148**, F1–F5 (2002).
24. Edwards, B., Allmann, B., Fah, D. & Clinton, J. Automatic computation of moment magnitudes for small earthquakes and the scaling of local to moment magnitude. *Geophys. J. Int.* **183**, 407–420 (2010).
25. Båth, M. Lateral inhomogeneities in the upper mantle. *Tectonophysics* **2**, 483–514 (1965).
26. Zaliapin, I. & Ben-Zion, Y. Y. Earthquake clusters in southern California. I: Identification and stability. *J. Geophys. Res.* **118**, 2847–2864 (2013).
27. Zaliapin, I. & Ben-Zion, Y. A global classification and characterization of earthquake clusters. *Geophys. J. Int.* **207**, 608–634 (2016).
28. McNamara, D. E. et al. Source modeling of the 2015 M_W 7.8 Nepal (Gorkha) earthquake sequence: implications for geodynamics and earthquake hazards. *Tectonophysics* **714–715**, 21–30 (2017).
29. Wells, D. L. & Coppersmith, K. J. New empirical relationships among magnitude, rupture length, rupture width, rupture area, and surface displacement. *Bull. Seismol. Soc. Am.* **84**, 974–1002 (1994).
30. Putnis, A., Jamtveit, B. & Austrheim, H. Metamorphic processes and seismicity: the Bergen Arcs as a natural laboratory. *J. Petrol.* **58**, 1871–1898 (2017).
31. Yardley, B. W. D. The role of water in the evolution of the continental crust. *J. Geol. Soc. Lond.* **166**, 585–600 (2009).
32. Munz, I. A., Yardley, B. W. D., Banks, D. & Wayne, D. Deep penetration of sedimentary fluids in basement rocks from Southern Norway—evidence from hydrocarbon and brine inclusions in quartz veins. *Geochim. Cosmochim. Acta* **59**, 239–254 (1995).
33. Austrheim, H. Fluid and deformation induced metamorphic processes around Moho beneath continent collision zones: Examples from the exposed root zone of the Caledonian mountain belt, W-Norway. *Tectonophysics* **609**, 620–635 (2013).

Acknowledgements This project has been supported by the European Union's Horizon 2020 Research and Innovation Programme under ERC Advanced Grant Agreement number 669972, 'Disequilibrium Metamorphism' ('DIME'; to B.J.), and by the Norwegian Research Council grant number 250661 ('HADES'; to F.R.). Y.B.-Z. acknowledges support from the National Science Foundation (grant EAR-1722561). The paper benefited from discussions with and comments by I. Zaliapin, J. Jackson, A. Putnis, S. Schmalholz, S. Xu, P. Meakin and J. Platt.

Reviewer information *Nature* thanks B. Yardley and the other anonymous reviewer(s) for their contribution to the peer review of this work.

Author contributions All authors designed this study. B.J. and Y.B.-Z. wrote the manuscript with input from F.R. and H.A., H.A. and B.J. conducted the field studies, F.R. designed the figures. Y.B.-Z. and F.R. derived the theoretical estimates of earthquake quantities motivated by the idea of 'seismic index' proposed by H.A.

Competing interests The authors declare no competing interests.

Additional information

Extended data is available for this paper at https://doi.org/10.1038/s41586-018-0045-y.

Correspondence and requests for materials should be addressed to B.J.

METHODS

Controls on lower-crustal stress levels. We used the flow law creep parameters for synthetic plagioclase aggregates for variable water contents from ref. [34]. Extended Data Fig. 1 shows the relations between temperature, strain rate and differential stress for water-poor plagioclase aggregates based on these experimental data. At 660–680 °C, the estimated temperature during seismic faulting in the Bergen Arcs, the maximum differential stress developing for a strain rate of 10^{-14} s^{-1} would be about 0.3 GPa, and clearly insufficient to cause brittle failure. Such strain rates would probably only apply within zones where strain was already localized. In a coherent crustal volume, the internal strain rate would be far less. Strain rates are estimated[7] at around 10^{-16} s^{-1} for the subducting Indian plate beneath eastern Tibet. Even if local strain rate increases should be able to push stress levels beyond what would be expected in coherent crustal slabs, or if the crustal temperature was lower than for the Bergen case so that the effective viscosity was higher, stresses much higher than 1 GPa would be unrealistic owing to the onset of Peierls creep[35], or even cataclastic flow[36].

Volume of damage produced by earthquakes. The step-by-step derivation of equation (3) and the calculation of the volume of rock damaged by earthquakes in the crust, V_{rd}, are detailed here. The total volume of rock damage produced by crustal earthquakes in the magnitude range $M_1 < M < M_2$ is given by equation (1). Each term in the integral of equation (1) is described below.

The density of events $n(M)$ in equation (1) is provided by the Gutenberg–Richter relationship, equation (2), where a and b are empirical constants. Assuming that each earthquake is approximately a circular rupture with radius r and surface area $A = \pi r^2$ that sustains a uniform strain drop $\Delta\varepsilon$, the seismic potency P_0 (moment divided by rigidity) is given by[21]

$$P_0 = (16/7)\,\Delta\varepsilon r^3 \tag{4}$$

The seismic potency and magnitude of earthquakes spanning a relatively small range (≤ 4) of magnitudes are related empirically by a relation of the type[23,24]

$$\log_{10} P_0 = dM + e \tag{5}$$

with constants d and e.

Combining equations (4) and (5), the radius of an earthquake with magnitude M in units of kilometres is:

$$r(M) = \left[\frac{7\times 10^{-5}}{16\Delta\varepsilon}\right]^{1/3} \times 10^{(dM+e)/3} \tag{6}$$

where the 10^{-5} factor accounts for the unit conversion of P_0 from km^2 cm to km^3. Using equation (6) for r and assuming again a circular crack such that $A(M) = \pi r^2$, we obtain

$$A(M) = \pi\left[\frac{7\times 10^{-5}}{16\Delta\varepsilon}\right]^{2/3} \times 10^{2(dM+e)/3} \tag{7}$$

The thickness of the damage zone t_{rd} is expected from fracture mechanics to scale linearly with the rupture radius[22].

$$t_{rd}(M) = \gamma r(M) \tag{8}$$

where the constant γ is proportional to the dynamic stress intensity factor and the ratio of stress drop over strength drop. For standard rupture velocity of 0.9 times the Rayleigh wave speed and a stress drop that is 10% of the strength drop, $\gamma \approx 10^{-2}$–10^{-3} (situations with relatively high initial stress leading to higher stress drop give higher γ values). Here we conservatively use $\gamma = 0.002$.

Combining equations (2), (7) and (8) leads to

$$A(M)\,t_{rd}(M)\,n(M) = \pi\gamma\left[\frac{7\times 10^{-5}}{16\Delta\varepsilon}\right] \times 10^{(d-b)M+e+a} \tag{9}$$

Integrating equation (1) using equation (9) gives an explicit relationship for the total volume of damage produced by earthquakes—that is, equation (3), where $\alpha = (d-b)\ln(10)$ and $\beta = \frac{\pi}{\alpha}\gamma 10^{a+e}\left(\frac{7\times 10^{-5}}{16\Delta\varepsilon}\right)$ are positive parameters and V_{rd} is in units of cubic kilometres per year per square kilometre of the Earth's surface in a seismically active region.

Observed b-values are typically around 1, while a-values vary considerably with space and time. We focus on deformation in subduction zones and seismically active continental regions and use average a and b values based on analysis of global earthquakes with depth shallower than 70 km during 1975–2015 in the Northern California Earthquake Data Center (NCEDC) catalogue[27]. Using figure 1 of ref. [27] and a b-value of 1, a representative intensity of events with $M > 0$ (10^a) in active subduction zones is 6 per year per square kilometre, corresponding to $a = \log_{10}(6) = 0.78$. This value is conservative because the NCEDC catalogue does not include numerous small events buried in the coda of larger events and noise. The results of ref. [27] indicate that about 50% of $M > 4$ events in subduction zones and continental transform regions are aftershocks. The fraction of events that are aftershocks increases as the event magnitude decreases[26,27], so we assume that about 75% of all events with $M > 0$ are aftershocks. The event intensity 10^a used below to estimate damaged rock volume by aftershocks is reduced accordingly by a factor of 0.75 from 6 to 4.5.

Analysis of earthquakes in southern California recorded by the regional network and borehole sensors indicates[23] that $d = 1$ and $e = -4.7$ for $M < 3.5$ while $d = 1.34$ and $e = -5.22$ for $M > 3.5$. Similar constants characterize earthquakes in other locations[24]. Inserting these constants d and e for magnitude ranges $0 < M < 3.5$ and $3.5 < M < 8.3$ into equation (9) and integrating, a more explicit expression of the volume of damaged rocks (in cubic kilometres per year per square kilometre of the Earth's surface at the seismically active region) is

$$V_{rd} = \int_{M_1}^{M_2} A(M)\,t_{rd}(M)\,n(M)\,\mathrm{d}M = \pi\gamma\left[\frac{7\times 10^{-5}}{16\Delta\varepsilon}\right] \times 10^{a} \int_{M_1}^{M_2} 10^{(d-b)M+e}\mathrm{d}M \tag{10}$$

and

$$V_{rd} = \pi\gamma\left[\frac{7\times 10^{-5}}{16\Delta\varepsilon}\right] 10^{a}\left\{\int_{0}^{3.5} 10^{-4.7}\mathrm{d}M + \int_{3.5}^{8.3} 10^{0.34M} \times 10^{-5.22}\mathrm{d}M\right\} \tag{11}$$

Evaluating equations (10) and (11) gives $V_{rd} = 1.2\times 10^{-5}$ km^3 per year per square kilometre of the Earth's surface in a seismically active region.

The fraction of lower-crust volume affected by earthquake ruptures (1.2%) is obtained using $10^a = 4.5$, $\Delta\varepsilon = 5\times 10^{-5}$ and the values of other constants mentioned in the text. The result is sensitive to the input parameters, but it is based on realistic values of earthquake intensities in active subduction zones (4.5 annual aftershocks with $M > 0$ per square kilometre), assumed lower and upper limits of aftershock magnitudes (0 and 8.3), average strain drop ($\Delta\varepsilon = 5\times 10^{-5}$), ratio of damage zone thickness to rupture radius $\gamma = 0.002$, and the fraction of aftershocks with hypocentres in the lower crust (1%). Reducing the lower magnitude limit will increase the rupture surface area but not change the estimated damage zone volume much; decreasing the upper magnitude limit from 8.3 to 7.8 will decrease the estimated volume of damaged rock by 32%. Changing the assumed average strain drop $\Delta\varepsilon = 5\times 10^{-5}$ to average strain drops of 5×10^{-4} and 5×10^{-6} will modify the estimated damage volume by factors of 0.21 and 4.64, respectively. Changing γ or the deformation timescale by a given factor (for example, 2) will modify the damage volume by the same factor. Thus, reasonable variations of these parameters will have only minor effects on the estimated lower-crust volume affected by earthquake ruptures.

Data availability. All of the data used are contained within the paper.

34. Rybacki, E. & Dresen, G. Deformation mechanism maps for feldspar rocks. *Tectonophysics* **382**, 173–187 (2004).
35. Azuma, S., Katayama, I. & Nakakuki, T. Rheological decoupling at the Moho and implications to Venusian tectonics. *Sci. Rep.* **4**, 4403 (2014).
36. Tullis, J. & Yund, R. The brittle–ductile transition in feldspar aggregates. An experimental study. *Int. Geophys.* **51**, 89–117 (1992).

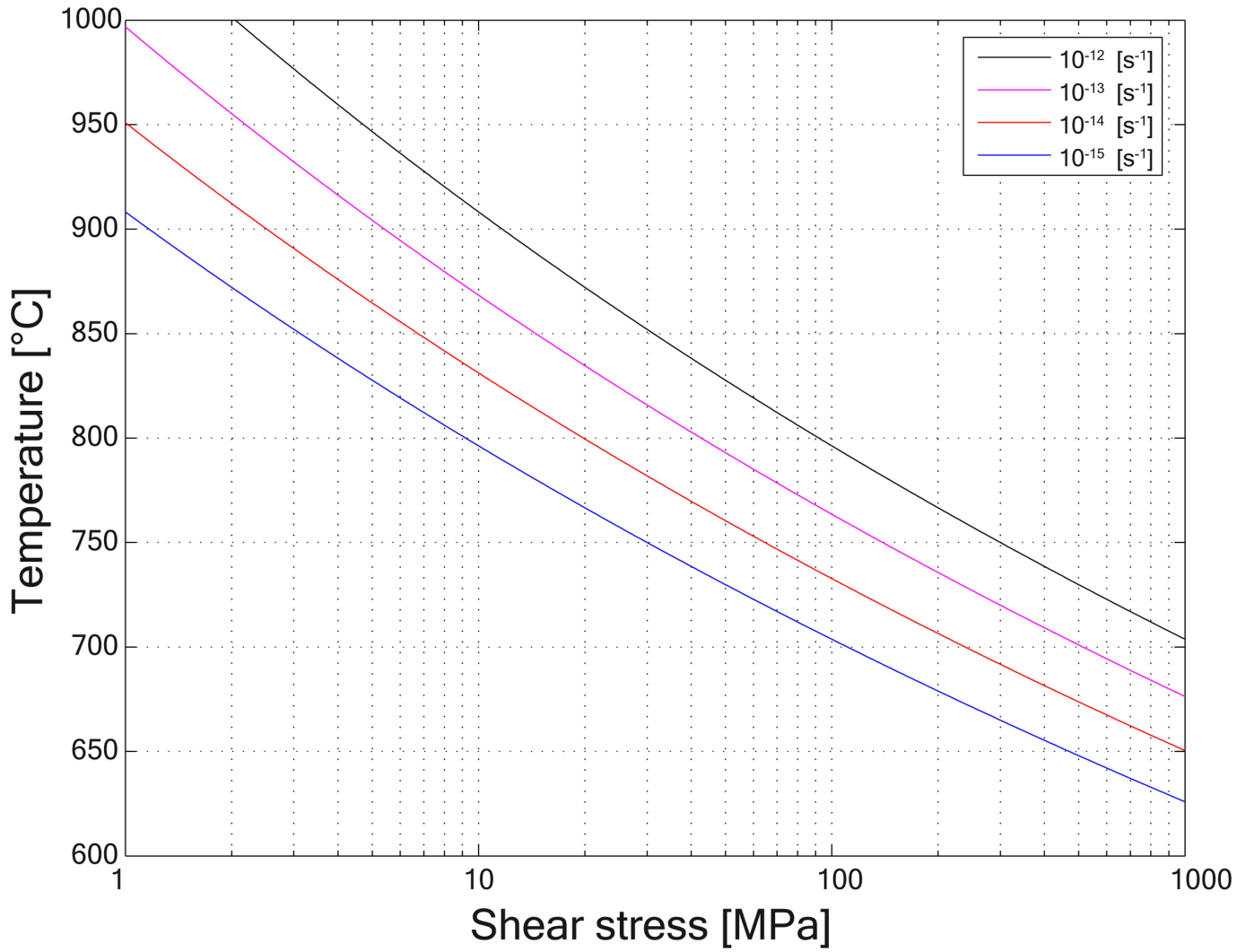

Extended Data Fig. 1 | Rheology of dry anorthite. Shear stress versus temperature diagram contoured with respect to strain rate.